Graphene Oxide–Based Hydrogels to Make Metal Nanoparticle–Containing Reduced Graphene Oxide–Based Functional Hybrid Hydrogels

ARTICLE *in* ACS APPLIED MATERIALS & INTERFACES · SEPTEMBER 2012

Impact Factor: 6.72 · DOI: 10.1021/am301373n · Source: PubMed

3 AUTHORS:

Bimalendu Adhikari
University of Toronto
24 PUBLICATIONS **714** CITATIONS
SEE PROFILE

Abhijit Biswas
Indian Association for the Cultivation of Science
8 PUBLICATIONS **194** CITATIONS
SEE PROFILE

Arindam Banerjee
Indian Association for the Cultivation of Science
131 PUBLICATIONS **3,161** CITATIONS
SEE PROFILE

ACS APPLIED MATERIALS & INTERFACES

Research Article

www.acsami.org

Graphene Oxide-Based Hydrogels to Make Metal Nanoparticle-Containing Reduced Graphene Oxide-Based Functional Hybrid Hydrogels

Bimalendu Adhikari, Abhijit Biswas, and Arindam Banerjee*

Department of Biological Chemistry, Indian Association for the Cultivation of Science, Jadavpur, Kolkata 700 032, India

Supporting Information

ABSTRACT: In this study, stable supramolecular hydrogels have been obtained from the assembly of graphene oxide (GO) in presence of polyamines including tris(aminoethyl)amine, spermine, and spermidine [biologically active molecule]. One of these hydrogels has been well characterized by various techniques including field-emission scanning electron microscopy (FE-SEM), transmission electron microscopy (TEM), atomic force microscopy (AFM), X-ray diffraction (XRD) study, and Raman spectroscopy. TEM and AFM studies of one of these hydrogels have revealed the presence of a network structure of cross-linked nanosheets. This suggests the supramolecular assembly of GO in the presence of polyamines using the acid−base type electrostatic interaction. In presence of a mild reducing agent (vitamin C), one of these GO hydrogels has been transformed into a reduced graphene oxide (RGO)-based hydrogel by a simple in situ reduction of GO sheets within the hydrogel matrix. Moreover, noble metal nanoparticle containing RGO based hybrid hydrogels have been obtained using in situ and simultaneous co-reduction of GO and noble metal precursors within the GO gel matrix. The elegance of this method is in situ, "green chemical" and simultaneous reduction of GO and metal salts within the hydrogel matrix to form RGO-based hybrid gel and concomitant stabilization of metal nanoparticles (MNPs) within the gel system. The nascently formed MNPs are homogeneously and uniformly distributed on the surface of the RGO nanosheets within the hybrid gel. Interestingly, this MNP containing RGO-based hybrid hydrogel matrix acts as a potential catalyst for the reduction of aromatic nitro to amino group. The catalyst (hybrid gel matrix) can be separated easily after the reaction and reused several times.

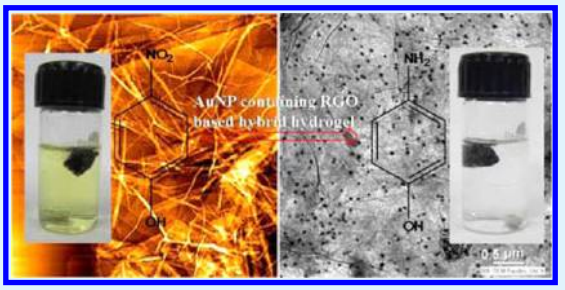

KEYWORDS: *graphene, hybrid material, hydrogel, self-assembly, nanoparticle, catalysis*

INTRODUCTION

Self-assembly is one of the most useful techniques to integrate various nanoscale building blocks into macroscopic materials with interesting properties.[1] These self-assembled superstructures exhibit novel collective physiochemical properties that are sometimes different from individual components and even from the bulk material. These superstructures are endowed with various practical applications.[2] Various noncovalent interactions including hydrogen bonding, aromatic stacking, electrostatic interactions, van der Waals interactions, and/or metal coordination interactions are involved in the assembly process.[3] One of the common self-assembling system is supramolecular gel and this is an attractive class of soft material comprising assembled network structure of the gelator molecules with a lot of interstitial space occupied by many immobilized solvent molecules.[4−6] These gels are endowed with many interesting and useful applications in different fields including optoelectronics, light harvesting, organic−inorganic hybrid materials, tissue engineering, and regenerative medicine.[4−6] These gelators are mainly based on small organic molecules.[4−6] Some of these gel matrices have been successfully exploited to make carbon-based nanomaterials containing hybrid gels.[7−9] Currently, graphene[10−19] and graphene oxide[20−25] based gels are an emerging field of nanomaterial research. GO-based hydrogels have been prepared by adding either polymers,[20,22] macromolecules,[21] small organic molecules,[20,23] or cations[12] into aqueous dispersion of GO. In these cases, the main driving forces for gelation are hydrogen bonding, $\pi-\pi$ interaction, or electrostatic interaction. Shi and his coworkers have developed GO based several hydrogels using polymers[19] and DNA.[20] Zhang and his coworkers have made a significant contribution on graphene-based hydrogelation[16,19] and they have discovered graphene oxide hydrogels by using glucono-δ-lactone.[25] Chemical attachment of cyclodextrin (CD) with GO and supramolecular host−guest complex formation have also been used to make graphene based hydrogels[26,27] and these hydrogels have been formed through the complexation between Pluronic and CD. There is also a report of the temperature-responsive GO-based hydrogel by adding a small amount of Pluronic into GO solution.[28] Previously, we have reported biomolecule (amino acid and nucleoside)-assisted hydrogelation of GO.[23]

The making of graphene-based various nanohybrid systems including graphene−AuNP,[29−48] graphene−AgNP,[49−52] and others[53−56]

Received: July 19, 2012
Accepted: September 12, 2012
Published: September 12, 2012

Scheme 1. Chemical Structures of Graphene Oxide, Reduced Graphene Oxide, and Polyamines As Mentioned Above; Photographs of GO-Based Supramolecular Hydrogels in the Presence of Polyamine: (a) Tris(aminoethyl)amine, (b) Spermine, and (c) Spermidine[a]

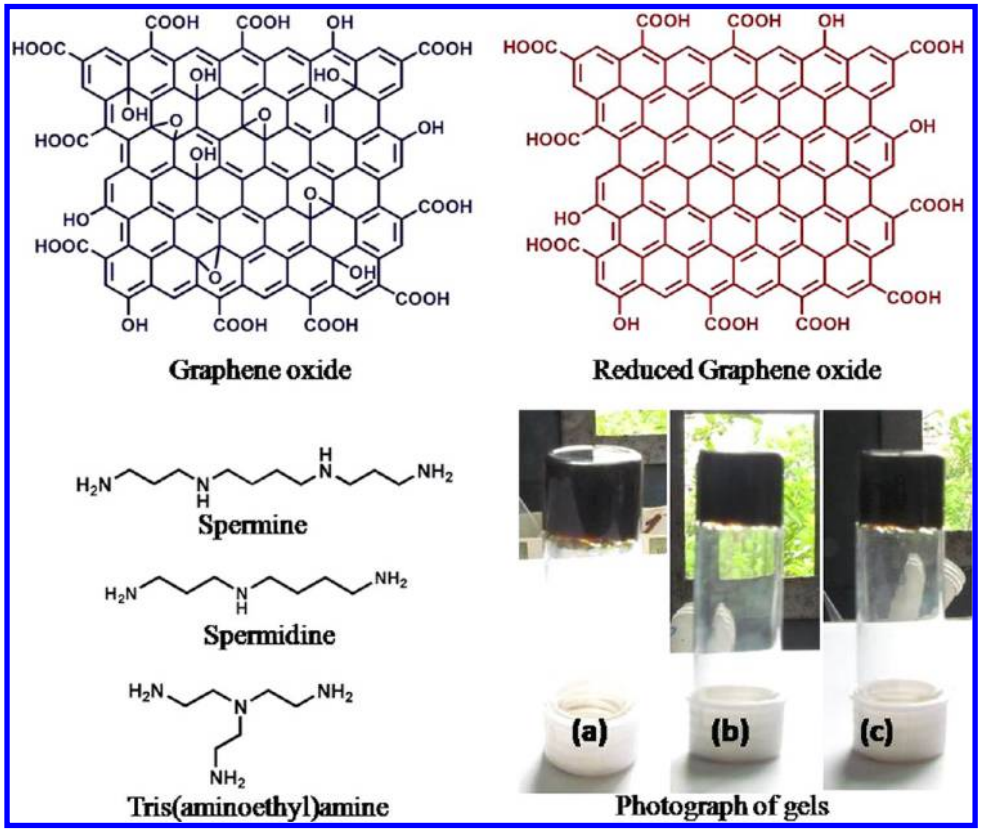

[a]These photographs indicate that they are gel-phase material and stable upon vial inversion.

has received very significant attention in current nanomaterial research because of their important applications in different fields including energy conversion, catalysis, fuel cells, and others. Kamat and coworkers have reported several nanohybrid system based on graphene–metal/metal oxide NPs.[29,31] Lin and coworkers have made graphene–NP hybrids for versatile applications including formic acid oxidation[53] and detection of organophosphate pesticide.[47] El-Shall and coworkers have demonstrated a synthesis of graphene–metal NPs hybrid using microwave irradiation.[36] To the best of our knowledge, there is no report of in situ and "green chemical" synthesis of noble metal (Au, Ag, and Pt) nanoparticles within the GO-based supramolecular hydrogel phase and the concomitant formation of reduced graphene oxide (RGO)-based functional hybrid hydrogel system for catalysis. In this report, we present the formation GO based supramolecular hydrogels in presence of a polyamine [tris(aminoethyl)amine/spermine/spermidine] and the in situ formation of metal NP containing RGO based functional hybrid hydrogel using a "green chemical" approach. Metal ions and GO are simultaneously reduced (using vitamin C) in a single step within the hydrogel phase in this reported method to form a nanohybrid system. Metal nanoparticles are uniformly fabricated on the surface of the RGO nanosheet to create a gel based nanohybrid system. Interestingly, this hybrid hydrogel matrix has been nicely exploited as a potential reusable catalyst for the reduction of aromatic nitro to amino group at room temperature.[57−62] The elegance of our hybrid system is that this hybrid material acts as a heterogeneous catalyst and it is very easily separable from the reaction mixture after the completion of the reaction and this makes reusability of this AuNP containing hybrid gel catalyst several times without losing its potency significantly.

EXPERIMENTAL SECTION

Synthesis of Graphene Oxide. Graphene oxide has been synthesized from natural graphite powder (<30 μm) by a modified Hummers method.

Preparation of GO-Based Hydrogel. Polyamines [tris(aminoethyl)-amine, spermine] have been dissolved in water to make a aqueous stock solution (1.2 mg/mL). In a typical experiment, 2.4 mg of GO has been dispersed in 1 mL of water by sonication and then 0.2 mL of polyamine has been added into it to obtain a GO-based hydrogel [minimum gelation concentration (mgc) 0.20%, w/v]. Sometimes, sonication assists the gel formation. It takes more time to form gels without sonication.

Preparation of RGO-Based Hydrogel. First, a stock solution (108 mg/mL) of ascorbic acid has prepared by dissolving it in water and then 0.2 mL of this solution has been added into the 0.8 mL aqueous dispersion of GO (9 mg/mL). The mixture has stirred for a few minutes. Then, 0.2 mL of tris(aminoethyl)amine (3.6 mg/mL) has been added into the mixture and the final mixture has sonicated occasionally for about 2 minutes followed by heating at 90 °C for 10 minutes. During heating, this GO gel has been transformed gradually to a reduced graphene oxide (RGO)-based gel within several minutes. The RGO gel has started to shrink with the progress of time. The gel has floated into the glass vial after a few minutes. Finally its volume has been reduced to 50% of its initial volume and a cylindrical-shaped reduced graphene oxide-based hydrogel has been obtained.

Synthesis of Metal Nanoparticles within RGO-Based Gel. At first, 50 μL of aqueous solution of metal salt ($HAuCl_4$/ $AgNO_3$/ K_2PtCl_4) (240 mg/mL) has been added into 0.8 mL of each set of aqueous dispersion of GO (12 mg/mL) and has been stirred and sonicated.

Scheme 2. Tentative Molecular Interaction between GO Sheets and Polyamines [(a) Tris(aminoethyl)amine and (b) Spermine] Showing an Acid−Base-Type Electrostatic Attraction to Form a Gel

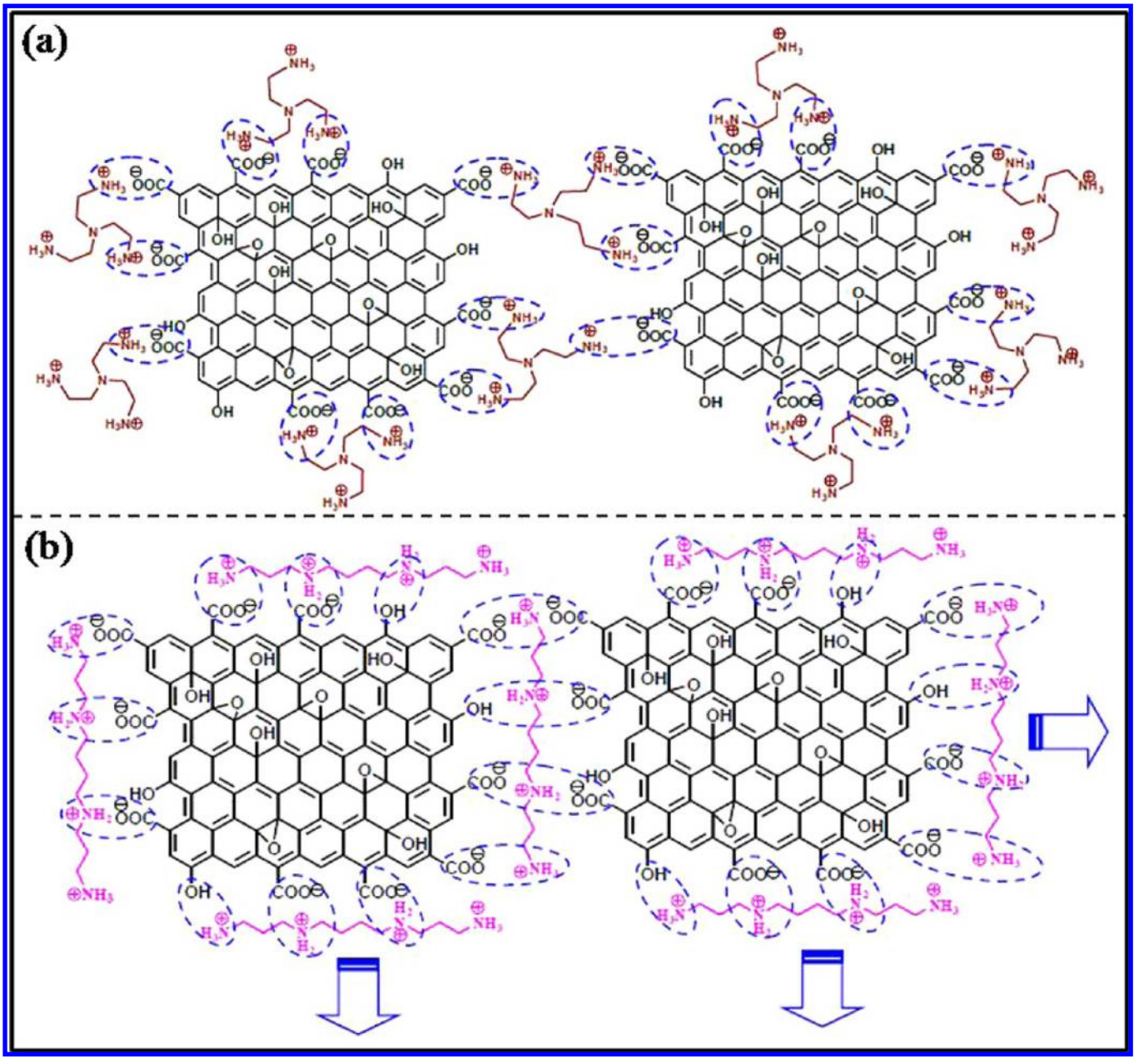

Then, into the mixture was added 0.2 mL of ascorbic acid (240 mg/mL), followed by the addition of 0.2 mL of tris(aminoethyl)amine (4.8 mg/mL). This mixture has been sonicated well. It was then heated well at 90 °C for 10 min. This has resulted in the formation of the corresponding metal nanoparticle containing RGO-based hybrid hydrogels. In this study, we have believed that metal ions have been reduced in situ by the ascorbic acid within the hydrogel matrix. AuNP containing RGO-based hybrid wet gel contains 0.90%, w/w Au.

Catalytic Reduction Study of 4-Nitrophenol and 4-Nitroaniline. The catalytic reduction study has been carried out in the presence of AuNP containing RGO-based hybrid hydrogel matrix in stirring condition. In a typical experiment, a fixed amount (1.32 g) of wet hybridgel (AuNP containing RGO based hybrid hydrogel) has been added into the mixture of 4-nitrophenol/4-nitroaniline (1.4×10^{-4} M), 5 mL of H_2O and $NaBH_4$ (0.1 M). The progress of the reaction has been recorded using UV-vis spectrometer at room temperature. As AuNP containing RGO-based hybrid wet gel contains 0.90%, w/w Au, 1.32 g of hybrid wet gel has 12 mg of AuNP and this (12 mg) amount of AuNP is responsible for the catalytic transformation.

Instrumentation. Field-emission scanning electron microscopy (FE-SEM). For the FE-SEM study, the tris(aminoethyl)amine-assisted GO-based hydrogel was placed on a microscope cover glass and the sample was freeze dried. The dried sample was then coated with platinum and the micrograph was recorded using an FE-SEM apparatus (JSM-6700F Jeol scanning microscope).

Transmission Electron Microscopy (TEM). Morphologies of the GO-based hydrogel, RGO-based hydrogel and noble metal nanoparticle (Au/Ag/Pt NP) containing RGO-based hybrid hydrogels have been studied by using TEM. These samples have been prepared by depositing a small amount of dilute gel phase material of the corresponding sample on a TEM grid (300 mesh size Cu grid) coated with Formvar and a carbon film. The grid has been allowed to dry under vacuum for 2 days. Images have been taken by a JEOL electron microscope.

Atomic Force Microscopy (AFM). Morphologies of the reported GO-based hydrogel and RGO-based hydrogel have been examined

dx.doi.org/10.1021/am301373n | ACS Appl. Mater. Interfaces 2012, 4, 5472−5482

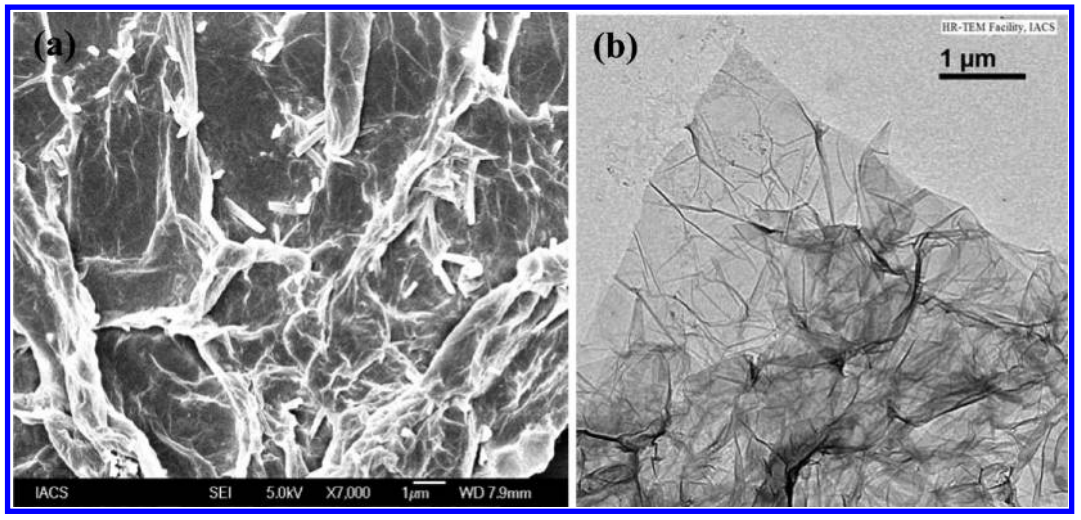

Figure 1. (a) FE-SEM and (b) TEM images of a GO-based hydrogel in the presence of tris(aminoethyl)amine suggesting the formation of three-dimensional network structure consisting of folded thin GO nanosheets.

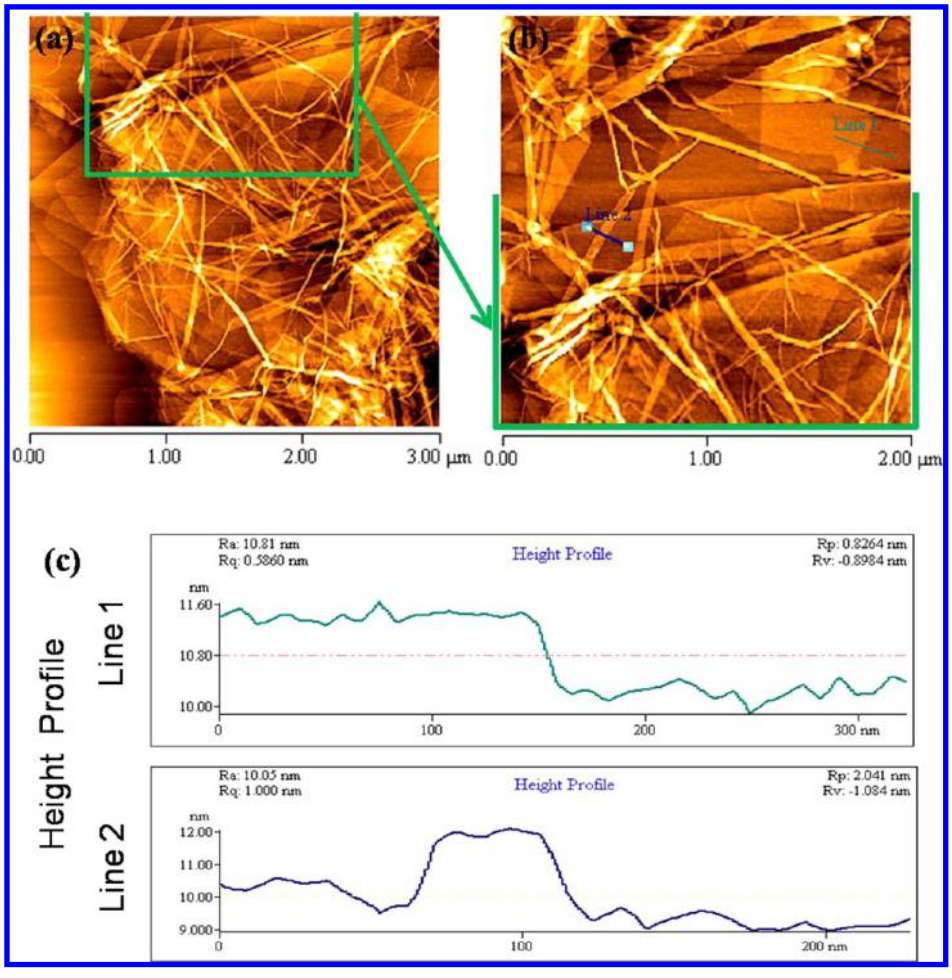

Figure 2. (a) AFM image of GO-based hydrogels in the presence of tris(aminoethyl)amine; (b) enlarged version of the image a (shown by green open rectangle); and (c) height profile diagram of the image b showing the presence of 1−2 layers of GO nanosheet(s).

using tapping-mode atomic force microscopy (AFM). AFM studies have been performed by placing a small amount of hydrogel on mica. The material has been then allowed to dry in air and then under vacuum for 2 days. Images have been recorded using an Autoprobe CP Base Unit di CP-II instrument (model AP-0100).

X-ray Diffraction (XRD). The XRD studies have been carried out using a dried GO-based hydrogel, RGO-based hydrogel, and Au nanoparticle containing RGO-based hybrid hydrogels by using an X-ray diffractometer (Bruker D8 Advance) equipped with a conventional Cu Kα X-ray radiation (λ = 1.54 Å) source and a Bragg diffraction setup (Seifert 3000P).

Raman Spectroscopy. For Raman spectra, the GO-based hydrogel and RGO-based hydrogel samples have been placed on a glass slide and then dried well. It has been measured by irradiating with laser

dx.doi.org/10.1021/am301373n | ACS Appl. Mater. Interfaces 2012, 4, 5472−5482

light at 632.81 nm in a Horiba Jobin Yvon instrument (LABRAM HR 800).

X-ray Photoelectron Spectroscopy (XPS). XPS analysis of dried pure GO and dried RGO gel have been carried on an ESCALAB MK II X-ray photoelectron spectrometer. For XPS experiment, RGO sample has been prepared first by removing impurities using extensive washing and then drying. Excess vitamin C, oxidized product of vitamin C, polyamine, and other soluble impurities present in the RGO gels have been eliminated by washing with excess water and ethanol. Then these samples have been dried under vacuum to obtain dried RGO gels.

UV/Vis Spectroscopy. UV/vis absorption spectra for the catalytic study have been recorded by using a Varian Cary 50 Bio UV/vis spectrophotometer.

HPLC Study. The product of the catalytic reduction was analysed by a HPLC system (Shimadzu) equipped with a diode array detector and an auto-sampler. Chramatographic separations were performed at room temperature using a polaris 5 C18-A2504×.6 mm (varian). A mobile phase composed of 80% MeOH and 20% water at a flow rate 0.9 mL min^{-1} was used.

RESULTS AND DISCUSSION

GO-Based Hydrogelation. A graphene oxide (GO) sheet can be regarded as a single-layer graphite sheet with various hydrophilic oxygenated functional groups such as hydroxyl, carboxyl, and epoxides (Scheme 1). Thus, GO sheets can be dispersed in water to form a stable colloidal dispersion. The carboxyl groups are ionized and can create electrostatic repulsion between two neighboring GO sheets. It is thought that electrostatic repulsion among the individual GO sheets actually prevents their aggregation in aqueous medium.[19] These groups (−OH, −COOH) can form hydrogen bonds with other molecules under appropriate conditions. So, the presence of other molecules with hydrogen bonds forming capability can be assembled with GO to form a hydrogel matrix.[19,22] In this report, various polyamines including tris(aminoethyl)amine, spermine, and spermidine [biologically active molecule] have been chosen to interact with graphene oxide (GO) sheets in water and GO sheets form stable supramolecular hydrogel in presence of any of these polyamines (Scheme 1). It can be mentioned that these hydrogels are neither thermoreversible nor mechanoreversible. The minimum gelation concentration (mgc) is 0.2%, w/v for tris(aminoethyl)amine and spermine and mgc is 0.25%, w/v for spermidine. These results indicate that the gelator GO is efficient. It can be mentioned that the required amount of a polyamine with respect to GO is very low (~10%, w/w). This suggests that the polyamine acts as a very good cross-linker between two GO sheets through hydrogen bonding and electrostatic interaction to form a gel (Scheme 2).

Biologically active polyamine, spermine is involved in cellular metabolism and it is found in all eukaryotic cells. At physiological pH, spermine exists as a protonated form with four positively charged amino groups that are separated by three, four and three carbon respectively. Spermidine is another polyamine that takes part in cellular metabolism. Tris(aminoethyl)amine is a branched polyamine with an N atom at the center. These polyamines are basic in nature and they exist as polyammonium ions at physiological pH. All three polyamines have N-containing basic functionalities that can accept protons from the COOH part of the GO sheets to participate in the acid-base type electrostatic attraction. Moreover, nitrogen (N)-containing functionalities of polyamines can form hydrogen bonds with hydroxyl groups (−OH) of GO sheets. Polyamine(s) can act as a strong binder between GO sheets through hydrogen bonding and acid−base type of interactions.

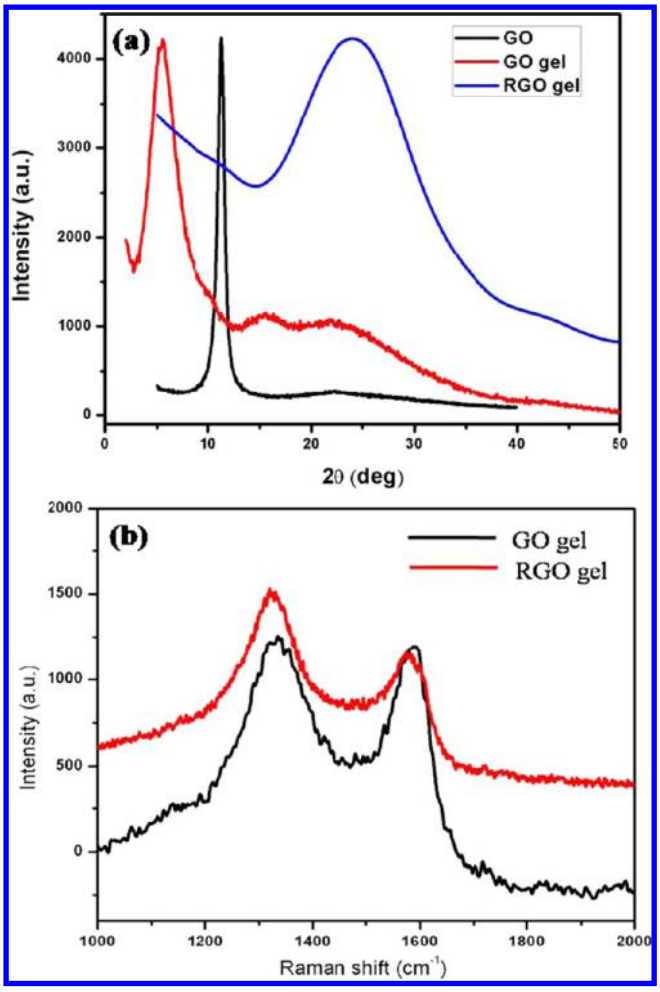

Figure 3. (a) XRD patterns of dried GO, tris(aminoethyl)amine induced GO gel, and reduced graphene oxide (RGO) gel as shown in the figure; (b) Raman spectra of GO gel and RGO gel as indicated.

Water molecules can be immobilized within the network obtained from the GO sheets and the binder molecules to form a hydrogel.

To get an insight about morphologies of the GO-based reported hydrogel, field-emission scanning electron microscopic (FE-SEM), transmission electron microscopic (TEM), and atomic force microscopic (AFM) studies have been carried out. For FE-SEM observation, the gel phase material (at mgc) has been placed on a microscopic glass slide and then freeze dried. The Figure 1a has shown a FE-SEM image of tris(aminoethyl)amine-assisted GO-based hydrogel. This reveals that nanostructured morphology is present in the supramolecular hydrogel. TEM image of the hydrogel has been shown in the Figure 1b and the image has shown the self-assembled large nanosheets. AFM study of the hydrogel (Figure 2) has also exhibited the formation of three-dimensional sheets. These nanosheets are 1-2 nm in width as it is evident from height profile diagram of AFM image. Moreover, these sheets are cross-linked with one another to form a large three dimensional networklike structure in presence of polyamines. These cross-linked sheets are also folded and it is evident from the figure TEM or AFM. It is worth mentioning that the black lines in TEM image are not nanofibers. These are appearing due to the folding nature of GO nanosheets (see Figure S1 in the supporting information). The driving forces for forming the large three-dimensional

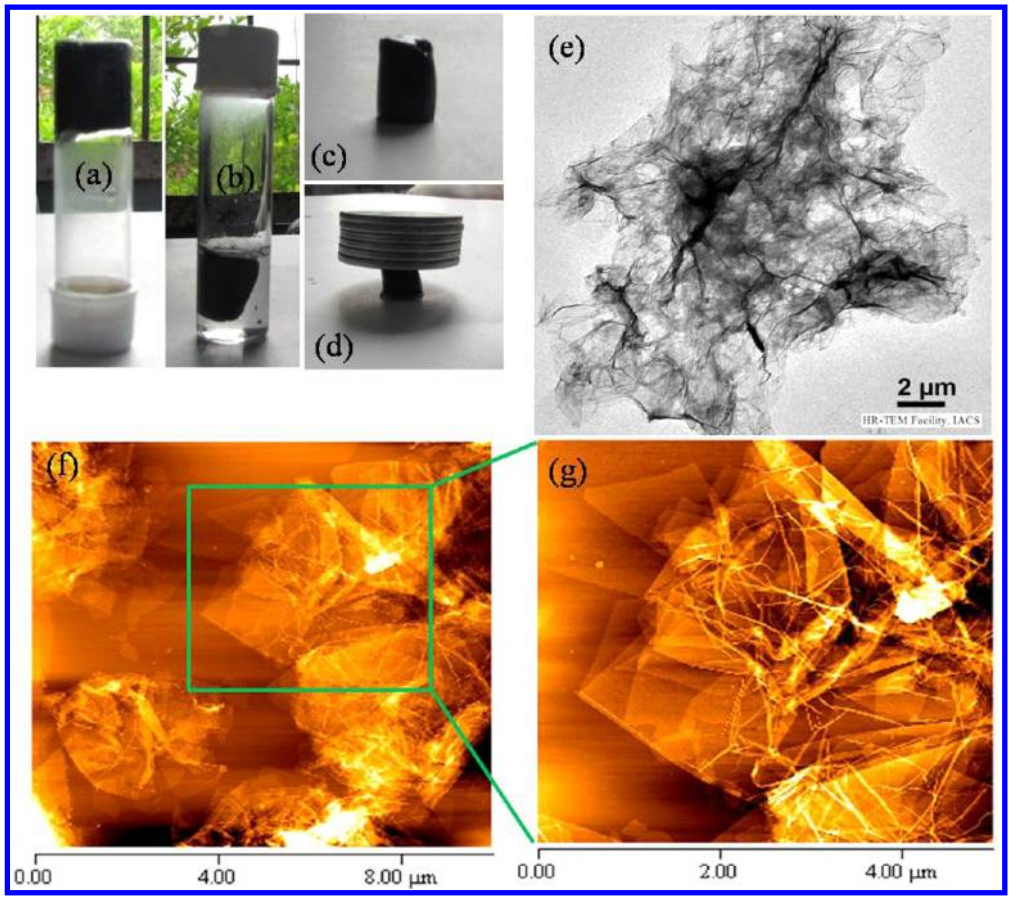

Figure 4. (a) Photographs of RGO-based hydrogel in the presence of tris(aminoethyl)amine, (b) shrinking of RGO gel in presence of heat, (c) piece of self-standing RGO gel, (d) load-bearing capacity of RGO gel; (e) TEM image RGO gel, (f) AFM image of RGO gel, and (g) an enlarged portion (green color marked region) of image f with a high resolution showing a network structure of cross-linked folded RGO nanosheets.

network-like structure are weak interactions, such as hydrogen bonding and acid-base type electrostatic interactions.

The GO hydrogel has been characterized using X-ray diffraction (XRD) study and Raman spectroscopic study. Figure 3a illustrates the X-ray diffraction (XRD) patterns of lyophilized GO and polyamine induced GO-based hydrogel. Pure GO shows a diffraction peak at 2θ = 11.26, corresponding to an inter-planar spacing of 7.85 Å.[22] XRD patterns of GO-based hydrogel shows a diffraction peak at 2θ = 5.55 (d spacing 15.90) and this is different from those of the pure GO. This is mainly due to the strong interaction between these two components (GO and polyamine).[22] This blue shift in diffraction peak from 2θ = 11.26 to 2θ = 5.55 is due to the absorption of polyamine on GO sheets and this has induced a slight lengthening of GO inter-planar spacing from 7.85 to 15.90 Å.

Raman spectroscopy gives a tool to characterize the carbon-based materials. Figure 3b represents the Raman spectrum of the dried GO hydrogel sample. Two fundamental vibrations have been observed, at 1591 and 1338 cm^{-1}, corresponding to the G band and D band of graphene oxide, respectively. The G band peak observed for GO-based hydrogel (1591 cm^{-1}) is shifted towards longer wavenumber compared to that of the raw graphite (1580 cm^{-1}).[61] This is due to the presence of isolated double bonds in GO that resonate at frequencies higher than that of the G-band of the graphite.[61]

The model structure of GO shows hydrophobic polyaromatic domains in its basal plane and hydrophilic hydroxyl and carboxylic acid groups along the edges. Polyamine [tris(amino ethyl) amine] molecule can act as a binder between GO sheets through multiple hydrogen bonding and acid-base type electrostatic attractions. As a result of that an extended layer type structure has been formed. This extended layer structure is further self-assembled using non-covalent interaction(s) to form a self-assembled robust 3D network structure as it is evident from morphological studies (AFM and TEM images).

Transformation of GO Gel into Reduced Graphene Oxide (RGO) Gel. Interestingly, this GO-based hydrogel can be successfully transformed into a reduced graphene oxide (RGO)-based hydrogel by in situ reduction of GO using vitamin C in presence of heat (80 °C) (Figure 4a). During heating, the gel material shrunk and the volume of the gel material decreased (Figure 4b, c). This shrinkage can be due to the fact of the reduction of GO to RGO accompanied by the decrease in the interlayer distance after the reduction of GO gel to RGO gel. Here, vitamin C acts as a good reducing agent to form GO to RGO within the gel matrix and without perturbing the gel network and breaking of the gel.[62] There are a few merits of using vitamin C as a reducing agent: (a) the entire reduction process does not produce any gaseous by-products and (b) vitamin C is a nontoxic environmentally reducing agent. As a result of that, a uniform aquatic gel has been formed without the formation of any gaseous by-products in course of the reduction of GO to RGO.

The RGO hydrogel has been characterized by, transmission electron microscopy (TEM), atomic force microscopy (AFM), X-ray diffraction (XRD) analysis, Raman spectroscopy and

dx.doi.org/10.1021/am301373n | ACS Appl. Mater. Interfaces 2012, 4, 5472−5482

X-ray photoelectron spectroscopy (XPS). Both TEM and AFM images (Figure 4e−g) of the RGO hydrogel show the presence of a 3D network comprising of self-assembled large nanosheets.

Figure 3a shows the XRD pattern of the dried RGO gel. The image vividly shows that the appearance of a very broad peak centered at 2θ = 24.08° and the complete disappearance of diffraction peak at 2θ = 5.55° (for GO gel). This clearly indicates the almost complete reduction of GO sheets to reduced graphene oxide (RGO) nanosheet in RGO gel with the removal of oxygen containing functionalities present in GO.

The Raman spectroscopic study of the RGO gel has been shown in the Figure 3b. This exhibits the G-band of dried RGO gel occurred at 1575 cm^{-1} and the intensity ratio of D/G band is more for RGO gel than that of GO gel. This suggests that more sp^2 domains are formed after the reduction of GO gel to RGO gel.[61]

The reduction of GO to RGO within the gel using vitamin C has also been confirmed by the XPS study. For the XPS experiment, excess vitamin C, oxidized product of vitamin C, polyamine and other soluble impurities present in the RGO gels have been removed by washing with a large amount of water and ethanol. Then, it has been dried to obtain dried RGO gels. Figure 5 has shown the C1s deconvoluted spectra of the RGO dried gel and GO powder. In case of GO, different peaks centered at 284.6, 286.7, 288.2, and 289.1 eV have been observed, corresponding to C═C and/or C−C in aromatic rings, C−OH (epoxy and alkoxy), C═O and O−C═O groups respectively. The C1s peak intensities centered at 286.7, 288.2, and 289.1 eV (especially 286.7) have been decreased significantly after the formation of RGO gel from the GO gel. This indicates that most of the oxygen-containing functional groups have been removed after the reduction using vitamin C.[16,61,62] On the other hand, there is an increase in intensity of the peak at 284.6 eV corresponding C═C and/or C−C in aromatic rings after the reduction of GO to the RGO. This suggests that the percentage of C═C and/or C−C in aromatic rings are increased significantly after the transformation of GO gel to RGO gel. This also indicates a restoration of the aromatic nature in the as-prepared RGO gel.

Although the RGO hydrogel contains about 99.8%, w/v water, its mechanical property is impressive. The semi-solid RGO based hydrogel material can tolerate weight and interestingly, hydrogel obtained from 50 mg GO can withstand upto 1.5 gm weight (Figure 4d) without any deformation of size and shape of this gel material. This is probably due to the following reasons. The mechanical stiffness of RGO itself is high due to the presence of polyaromatic domains in basal plane of RGO. Moreover, during gel formation RGO sheets are interacting strongly with the binder (polyamine) to form self-assembled extended network structure in a gel phase material. After reduction, RGO gel became much harder compared to the GO gel as this gel (RGO gel) has good load-bearing capacity. The low hydrophilicity of RGO (compared to GO) can not affect the gel formation, but, it can affect their properties.

Metal Nanoparticles Containing RGO-Based Hydrogel. RGO-based gels have a lot of interstitial space among the three-dimensional cross-linked network system to provide a wonderful opportunity for nucleation and growth of nanoparticles within the gel matrix.[6] Though there are several examples of the preparation of metal NPs on the graphene surface to make nanohybrid systems,[29−56] there is a rare example for the in situ and "green chemical" synthesis of noble metal nanoparticles (Au, Ag and Pt NPs) within the RGO-based

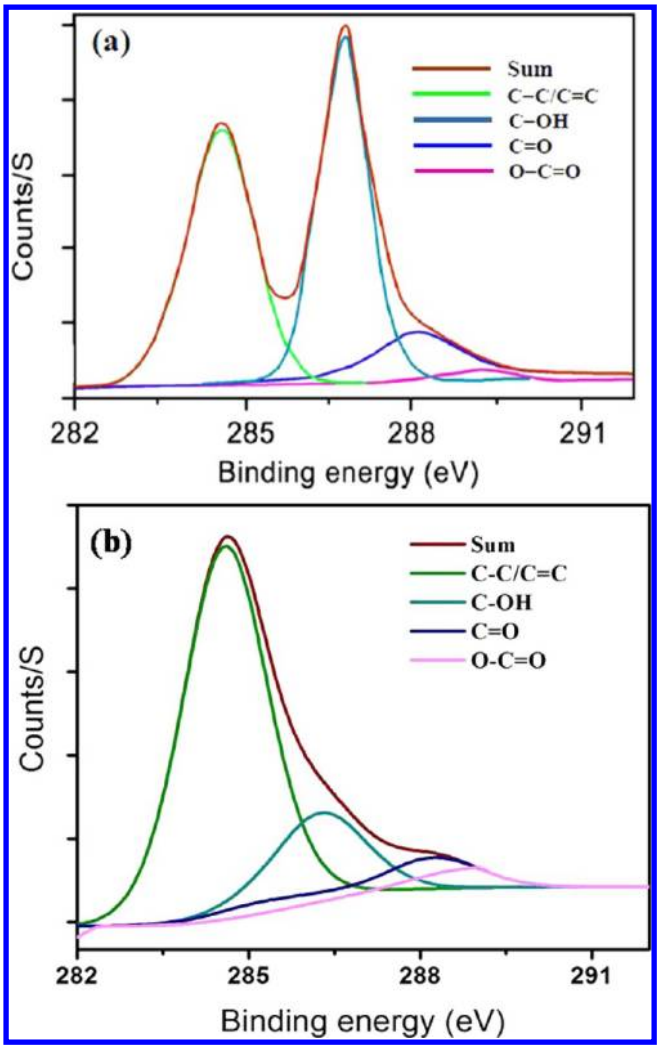

Figure 5. C1s XPS spectra of (a) graphene oxide and (b) dried RGO gel.

supramolecular hydrogel matrix to create MNP fabricated reduced graphene oxide (RGO) nanosheets to the best of our knowledge.[16] In this study, the RGO hydrogel has been functionalized and the corresponding RGO/noble metal nanoparticles hybrid hydrogels have been obtained after the co-reduction of noble metal ions and GO to form RGO-based MNP containing hybrid hydrogel in the presence of vitamin C.

Formation and characterization of metal nanoparticles within the RGO-based gel have been established using X-ray diffraction (XRD) study and transmission electron microscopy (TEM). The XRD pattern for the AuNP containing RGO-based hybrid dried gel has been shown in the Figure 6a. There are diffraction peaks at 2θ= 23, 38.3, 44.4, 64.8, 77.7, and 82.1 (Figure 6a). The first diffraction peak at 2θ = 23° suggests the reduction of GO sheet to form RGO sheet in the gel. Other diffraction peaks at 2θ = 38.3, 44.4, 64.8, 77.7, and 82.1° are consistent with those for Au nanoparticles and they correspond to the (111), (200), (220), (311), and (222) Miller indices of Au, respectively.

Various TEM studies have been carried out using the Au, Ag and Pt NPs containing RGO-based hybrid gels to examine the morphology of each of these noble metal nanoparticles containing RGO based hybrid gels. These TEM images (Figure 6b−d) have revealed that fabrication of MNPs on the RGO

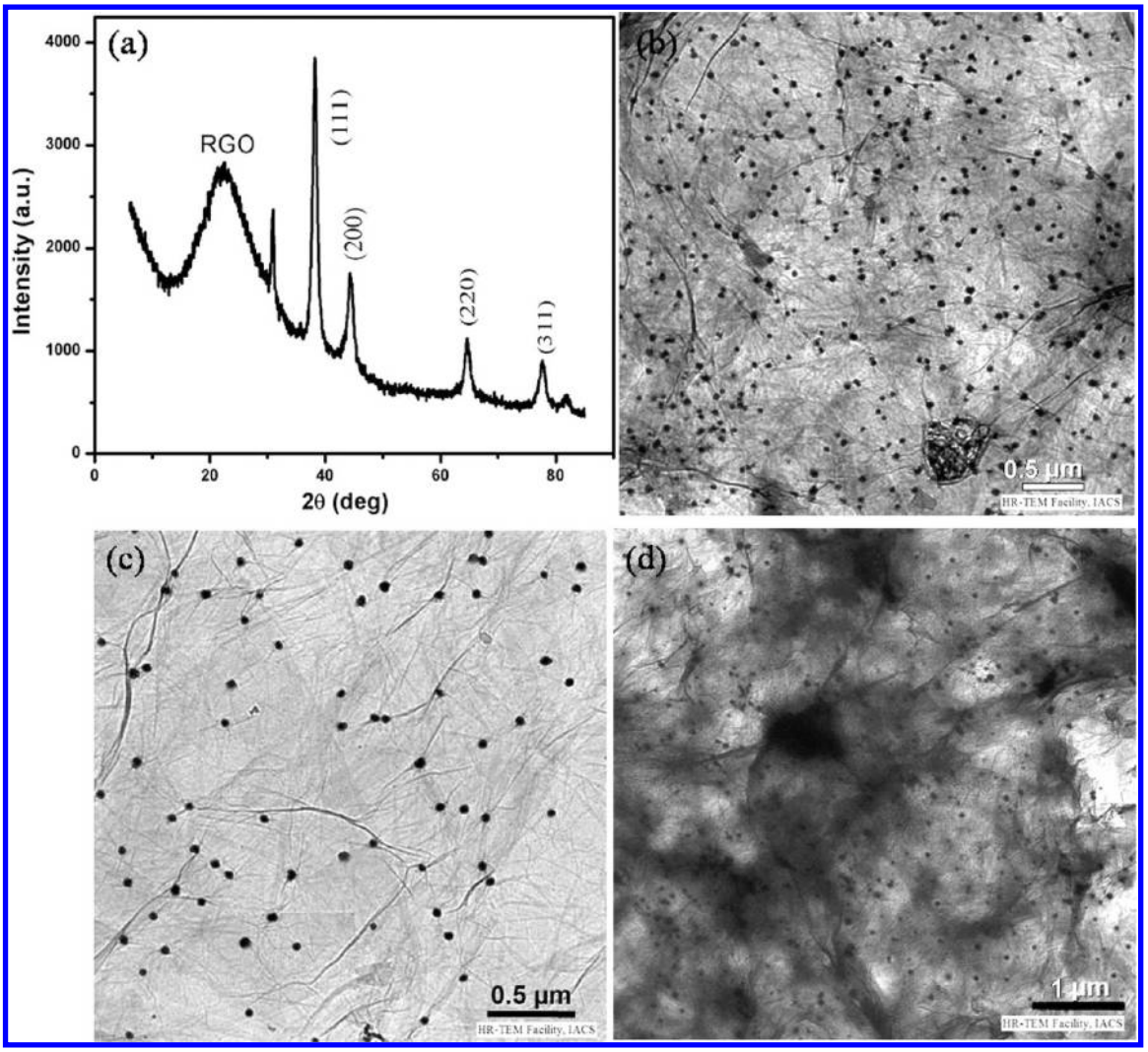

Figure 6. (a) XRD pattern of AuNP containing RGO-based hybrid hydrogel; TEM images of (a) Au, (b) Ag, and (c) Pt nanoparticle containing RGO-based hybrid hydrogels.

nanosheets within the hybrid gel system has been occurred uniformly. Diameters of Au, Ag, and Pt nanoparticles have been determined from their respective TEM images and it has been found to be 50 nm, 45 nm and 55 nm for Au, Ag and Pt nanoparticles respectively. The uniform and homogenous decoration of metal nanoparticle on the reduced graphene oxide nanosheets can be due to in situ reduction of metal salts within the gel matrix.

Catalytic Property of Hybrid Hydrogel. The catalytic property of Au nanoparticle containing RGO based hybrid hydrogel matrix has been investigated for the transformation of aromatic nitro to amino group: (i) reduction of *p*-nitrophenol by $NaBH_4$ and (ii) p-nitroaniline by $NaBH_4$ (Figures 7).[57−60] For catalytic experiment, freshly prepared aqueous solution of $NaBH_4$ has been added into diluted aqueous solution of *p*-nitrophenol or p-nitroaniline at room temperature. In the case of reduction of *p*-nitroaniline, a decrease in the UV-vis absorption peak at 381 nm has been observed with the decrease in intensity of the light greenish color (see Figure S2 in the supporting information). A color change from light yellow to yellowish green has been observed after the addition of $NaBH_4$ in *p*-nitrophenol. This color change is due to the formation of phenoxide ion and not due to the reduction of nitro to amino group, as in absence of any catalyst the transformation of nitro to amino group does not occur at all using $NaBH_4$ as a reducing agent. For catalytic study, the absorption spectra of the respective solutions in presence of such hybrid hydrogel (containing Au NPs) catalyst have been monitored with respect to time using UV-visible spectroscopy and these results have been presented in Figure 8. As shown in the figure 8, the decrease in intensity of the 400 nm peak for *p*-nitrophenol has been observed with the progress of the time in the presence of hydrogel catalyst. After completion of the reduction, yellow greenish solution of p-nitrophenol has been completely changed to colorless solution (see Figures 7). In the case of the control reaction, in the absence of hydrogel catalyst, there is no color change of *p*-aminophenol solution and no change in UV−vis peak position has been observed. The depletion of the 400 nm peak has been used to determine the rate constant of such a catalyzed reaction. For this purpose, a plot of $-\ln A_{400}$ against time has been drawn (see Figure S3 in the Supporting Information) and the rate constant (k) value has been determined from the slope of the straight line. It has been found to be 8.5×10^{-3} min^{-1}.

The catalytic study has been monitored by using the high performance liquid chromatography (HPLC) (see Figure S4 in

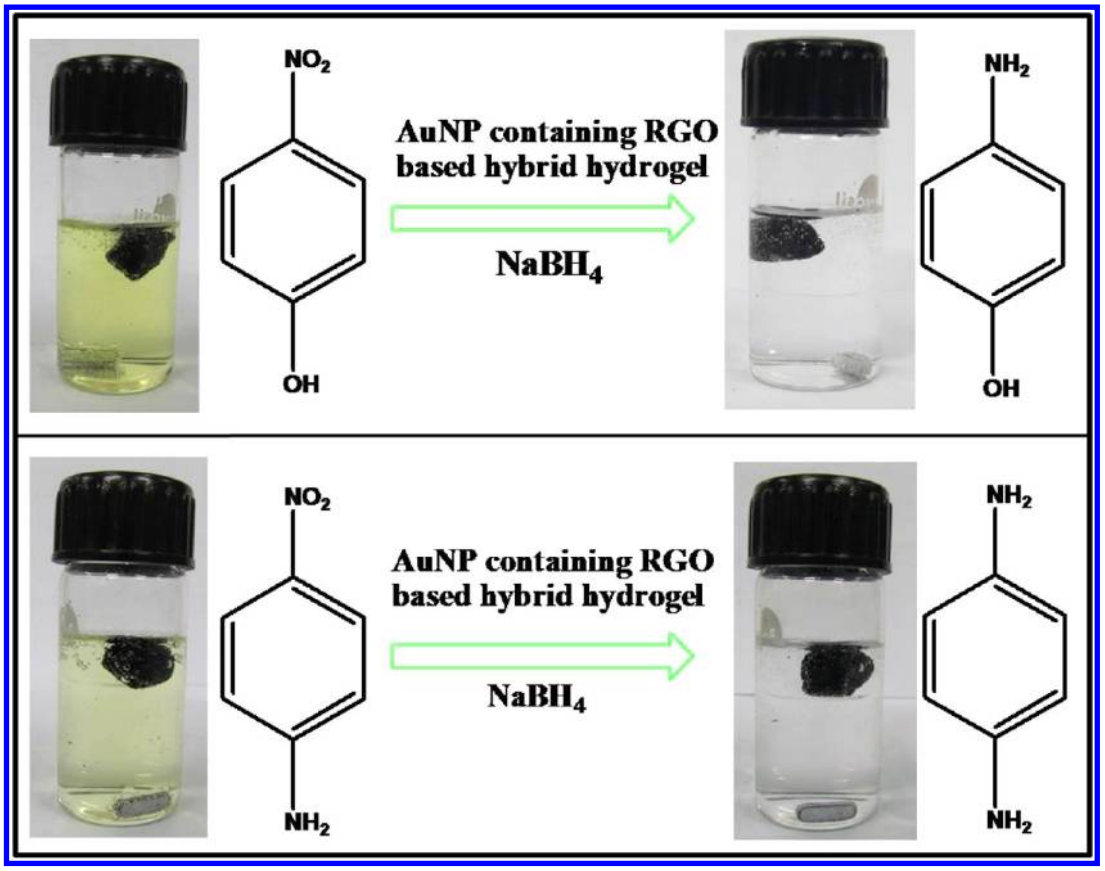

Figure 7. Schematic representation of AuNP containing RGO-based hybrid hydrogel catalyzed hydrogenation reactions: reduction of *p*-nitrophenol to *p*-aminophenol (above) and *p*-nitroaniline to *p*-diphenyleneamine (below) under stirring condition.

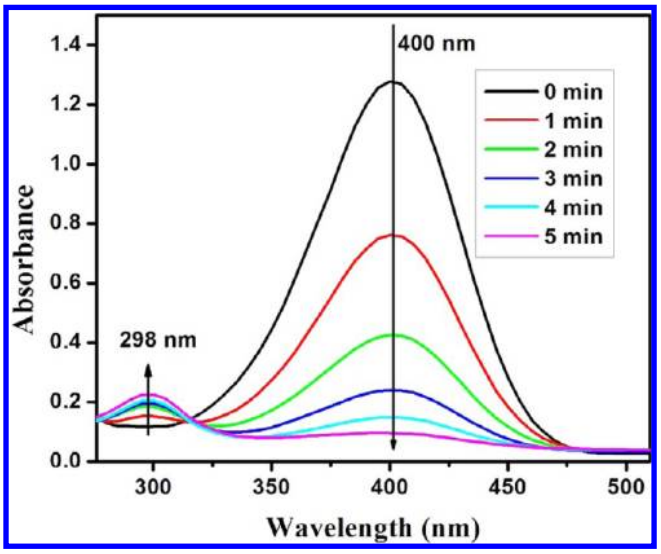

Figure 8. Successive UV−vis absorption spectra of the reduction of 4-nitrophenol by $NaBH_4$ in the presence of AuNP containing RGO-based hybrid hydrogel as a catalyst.

the Supporting Information). The appearance of the product p-aminophenol during the process of the reduction of *p*-nitrophenol with $NaBH_4$ using the hybrid RGO gel catalyst has been monitored at different time intervals. The HPLC retention time at 4.3 min and 3.1 min are corresponding to the substrate *p*-nitrophenol and the product *p*-aminophenol respectively. At time $t = 0$ (initially) only one peak has been observed at 4.3 min (retention time) for *p*-nitrophenol. The new peak with a retention time of 3.1 min has started appearing with the progress of the reduction and the peak corresponding to 4.3 min retention time has started gradually decreasing with the progress of time. At the end ($t = 6$ min) only one peak has been observed with a retention time of 3.1 min. This HPLC analysis clearly suggests the presence of the product *p*-aminophenol.

It can be mentioned that the rate constant value obtained under the present experimental condition is dependent on the amount of the Au nanoparticle loaded hydrogel catalysts used and the rate of the reactions can be increased further, if the amount of catalyst or the Au-loading capacity is increased. Interestingly, it has been observed that the catalytic property of the above AuNP-loaded hydrogel is not deteriorated significantly on repeated use. We have repeated the above reactions four times using the same catalyst under similar reaction conditions. The rate constant (k) value of the respective reaction has not been decreased significantly with respect to the different cycles. The use of this catalyst has several following merits: (i) the hydrogel catalyst can be kept inside the reaction mixture for catalytic study and easily separated after completion of the reaction, because the RGO-based hybrid gel is extremely hydrophobic in nature, (ii) it is easy to monitor the progress of the reduction as the time dependent UV-vis spectra can be easily monitored with the progress of the catalytic reaction without any overlapping absorption band originating from the AuNP catalyst; (iii) the hydrogel catalyst can be reused for further reduction; (iv) hybrid hydrogel catalyst is very easy to prepare and it is also inexpensive; (v) catalyst is very active towards reduction because both of these catalytic transformations take only a few minutes

dx.doi.org/10.1021/am301373n | *ACS Appl. Mater. Interfaces* 2012, 4, 5472−5482

(5 minutes) to complete. So, our AuNP containing RGO gel based catalyst is easily separable after the completion of the reaction and it takes much less time for the reduction compared to other regularly synthesized AuNP based catalytic system.[60,63−65] Particularly, separation of catalytic nanoparticles from the reaction mixture and regeneration of their catalytic properties are very difficult and they are becoming big issues in the industry.

In this study, RGO nanosheets within the hydrogel act as an excellent support for anchoring the AuNPs. These AuNPs act as a good catalyst for the reductive transformation. Here, it is expected that *p*-nitrophenol or p-nitroaniline can be adsorbed on the surface of RGO via $\pi-\pi$ stacking interactions. This results in the increase in effective concentration of *p*-nitrophenol or *p*-nitroaniline within the catalytic gel system containing RGO and AuNPs and this leads to the good catalytic activity due to the close proximity between the substrate and catalyst.

CONCLUSION

Polyamine [tris(aminoethyl)amine, spermine, and spermidine] induced graphene oxide based new supramolecular hydrogels have been discovered. Morphological studies of these hydrogels suggest the presence of a network structure of cross-linked nano-sheets. One of these GO hydrogels has been successfully transformed into reduced graphene oxide (RGO) based hydrogel by simple in situ reduction of GO sheet using vitamin C. Moreover, noble metal (Au, Ag and Pt) nanoparticle containing RGO based functional hybrid hydrogels have been obtained in situ by simultaneous co-reduction of GO and noble metal precursors within the GO gel matrix using a "green chemical" method in presence of vitamin C. These metal nanoparticles have been uniformly decorated on the surface of the RGO nanosheets to create a hybrid system. Interestingly, AuNP containing RGO-based hybrid hydrogel matrix has been successfully utilized as an efficient catalyst for the reduction of aromatic nitro to amino group. This as-prepared hybrid hydrogel catalyst has several advantages: (i) hybrid hydrogel catalyst is very easy to separate out from the reaction mixture after the reduction, (ii) catalyst is reusable for several times, (iii) it takes short time (~5 min), and (iv) it is easy to prepare and inexpensive. Interestingly, the simultaneous reduction of GO and metal ions has occurred within the hydrogel matrix to make a new hybrid system. This has the merit of making nascently formed metal nanoparticle trapped within the porous 3D network structure of the gel matrix and to assist the uniform deposition of metal nanoparticles on the surface of the RGO sheet. The overall process helps the reusability of the catalyst (hybrid gel) as AuNP containing RGO is immiscible with water and the aqueous solution can go into the gel matrix easily. The preparation of noble metal nanoparticle containing RGO-based nanohybrid system within the gel matrix using a single step, 'green chemical" approach can be extended to make other gel-based functional nanohybrid systems with different applications.

ASSOCIATED CONTENT

Supporting Information

Schematic presentation for the self-assembly of graphene oxide, UV−vis spectral change of *p*-nitroaniline during catalytic reduction, pseudo-first-order plot for the reduction of *p*-nitrophenol, and catalytic study using HPLC analyses. This material is available free of charge via the Internet at http://pubs.acs.org/.

AUTHOR INFORMATION

Corresponding Author

*Fax: +91-332473-2805. E-mail: bcab@iacs.res.in.

Notes

The authors declare no competing financial interest.

ACKNOWLEDGMENTS

B.A. and A.B. thank the CSIR, New Delhi, India, for financial assistance. We also acknowledge the DST project, Govt. of India for the financial support.

REFERENCES

(1) Vanmaekelbergh, D. *Nano Today* **2011**, *6*, 419−437.
(2) Mann, S. *Nat. Mater.* **2009**, *8*, 781−792.
(3) Lehn, J.-M. *Proc. Natl. Acad. Sci. U.S.A.* **2002**, *99*, 4763−4768.
(4) Hirst, A. R.; Escuder, B.; Miravet, J. F.; Smith, D. K. *Angew. Chem., Int. Ed.* **2008**, *47*, 8002−8018.
(5) Zhang, Y.; Kuang, Y.; Gao, Y.; Xu, B. *Langmuir* **2011**, *27*, 529−537.
(6) Banerjee, S.; Das, R. K.; Maitra, U. *J. Mater. Chem.* **2009**, *19*, 6649−6687.
(7) Samanta, S. K.; Pal, A.; Bhattacharya, S.; Rao, C. N. R. *J. Mater. Chem.* **2010**, *20*, 6881−6890.
(8) Tian, Y.; Zhang, L.; Duan, P.; Liu, F.; Zhang, B.; Liu, C.; Liu, M. *New J. Chem.* **2010**, *34*, 2847−2852.
(9) Adhikari, B.; Nanda, J.; Banerjee, A. *Chem.—Eur. J.* **2011**, *17*, 11488−11496.
(10) Xu, Y.; Sheng, K.; Li, C.; Shi, G. *ACS Nano* **2010**, *4*, 4324−4330.
(11) Worsley, M. A.; Pauzauskie, P. J.; Olson, T. Y.; Biener, J.; Satcher, J. H., Jr; Baumann, T. F. *J. Am. Chem. Soc.* **2010**, *132*, 14067−14069.
(12) Jiang, X.; Ma, Y.; Li, J.; Fan, Q.; Huang, W. *J. Phys. Chem. C* **2010**, *114*, 22462−22465.
(13) Cong, H.-P.; Ren, X.-C.; Wang, P.; Yu, S.-H. *ACS Nano* **2012**, *6*, 2693−2703.
(14) Lin, Y.; Ehlert, G. J.; Bukowsky, C.; Sodano, H. A. *ACS Appl. Mater. Interfaces* **2011**, *3*, 2200−2203.
(15) Yang, X.; Qiu, L.; Cheng, C.; Wu, Y.; Ma, Z.-F.; Li, D. *Angew. Chem., Int. Ed.* **2011**, *50*, 7325−7328.
(16) Sui, Z.; Zhang, X.; Lei, Y.; Luo, Y. *Carbon* **2011**, *49*, 4314−4321.
(17) Chen, W.; Yan, L. *Nanoscale* **2011**, *3*, 3132−3137.
(18) Tang, Z.; Shen, S.; Zhuang, J.; Wang, X. *Angew. Chem., Int. Ed.* **2010**, *49*, 4603−4607.
(19) Zhang, X.; Sui, Z.; Xu, B.; Yue, S.; Luo, Y.; Zhan, W.; Liu, B. *J. Mater. Chem.* **2011**, *21*, 6494−6497.
(20) Bai, H.; Li, C.; Wang, X.; Shi, G. *J. Phys. Chem. C* **2011**, *115*, 5545−5551.
(21) Xu, Y.; Wu, Q.; Sun, Y.; Bai, H.; Shi, G. *ACS Nano* **2010**, *4*, 7358−7362.
(22) Tung, V. C.; Kim, J.; Cote, L. J.; Huang, J. *J. Am. Chem. Soc.* **2011**, *133*, 9262−9265.
(23) Adhikari, B.; Biswas, A.; Banerjee, A. *Langmuir* **2012**, *28*, 1460−1469.
(24) Cheng, Q.-Y.; Zhou, D.; Gao, Y.; Chen, Q.; Zhang, Z.; Han, B.-H. *Langmuir* **2012**, *28*, 3005−3010.
(25) Huang, H.; Lu, S.; Zhang, X.; Shao, Z. *Soft Matter* **2012**, *8*, 4609−4615.
(26) Zu, S. Z.; Han, B. H. *J. Phys. Chem. C* **2009**, *113*, 13651−13657.
(27) Liu, J.; Chen, G.; Jiang, M. *Macromolecules* **2011**, *44*, 7682−7691.
(28) Sahu, A.; Choi, W. I.; Tae, G. *Chem. Commun.* **2012**, *48*, 5820−5822.
(29) Kamat, P. V. *J. Phys. Chem. Lett.* **2011**, *2*, 242−251.
(30) Huang, X.; Qi, X.; Boey, F.; Zhang, H. *Chem. Soc. Rev.* **2012**, *41*, 666−686.
(31) Muszynski, R.; Seger, B.; Kamat, P. V. *J. Phys. Chem. C* **2008**, *112*, 5263−5266.

(32) Xu, C.; Wang, X.; Zhu, J. *J. Phys. Chem. C* **2008**, *112*, 19841−19845.
(33) Goncalves, G.; Marques, P. A. A. P.; Granadeiro, C. M.; Nogueira, H. I. S.; Singh, M. K.; Gracio, J. *Chem. Mater.* **2009**, *21*, 4796−4802.
(34) Kong, B.-S.; Geng, J.; Jung, H.-T. *Chem. Commun.* **2009**, 2174−2176.
(35) Hong, W.; Bai, H.; Xu, Y.; Yao, Z.; Gu, Z.; Shi, G. *J. Phys. Chem. C* **2010**, *114*, 1822−1826.
(36) Hassan, H. M. A.; Abdelsayed, V.; Khder, A. E. R. S.; AbouZeid, K. M.; Terner, J.; El-Shall, M. S.; Al-Resayes, S. I.; El-Azhary, A. A. *J. Mater. Chem.* **2009**, *19*, 3832−3837.
(37) Xiong, Z.; Zhang, L. L.; Ma, J.; Zhao, X. S. *Chem. Commun.* **2010**, *46*, 6099−6101.
(38) Liu, J.; Fu, S.; Yuan, B.; Li, Y.; Deng, Z. *J. Am. Chem. Soc.* **2010**, *132*, 7279−7281.
(39) Fu, X.; Bei, F.; Wang, X.; O'Brien, S.; Lombardi, J. R. *Nanoscale* **2010**, *2*, 1461−1466.
(40) Xiang, J.; Drzal, L. T. *ACS Appl. Mater. Interfaces* **2011**, *3*, 1325−1332.
(41) Zhang, H.; Chen, S.; Quan, X.; Yu, H.; Zhao, H. *J. Mater. Chem.* **2011**, *21*, 12986−12990.
(42) Aravind, S. S. J.; Eswaraiah, V.; Ramaprabhu, S. *J. Mater. Chem.* **2011**, *21*, 17094−17097.
(43) Yang, X.; Xu, M.; Qiu, W.; Chen, X.; Deng, M.; Zhang, J.; Iwai, H.; Watanabe, E.; Chen, H. *J. Mater. Chem.* **2011**, *21*, 8096−8103.
(44) He, F.-A.; Fan, J.-T.; Song, F.; Zhang, L.-M.; Chan, H. L.-W. *Nanoscale* **2011**, *3*, 1182−1188.
(45) Jeon, K.-J.; Lee, Z. *Chem. Commun.* **2011**, *47*, 3610−3612.
(46) Lu, G.; Li, H.; Liusman, C.; Yin, Z.; Wu, S.; Zhang, H. *Chem. Sci.* **2011**, *2*, 1817−1821.
(47) Wang, Y.; Zhang, S.; Du, D.; Shao, Y.; Li, Z.; Wang, J.; Engelhard, M. H.; Li, J.; Lin, Y. *J. Mater. Chem.* **2011**, *21*, 5319−5325.
(48) Zhang, N.; Qiu, H.; Liu, Y.; Wang, W.; Li, Y.; Wang, X.; Gao, J. *J. Mater. Chem.* **2011**, *21*, 11080−11083.
(49) Tang, X.-Z.; Cao, Z.; Zhang, H.-B.; Liu, J.; Yu, Z.-Z. *Chem. Commun.* **2011**, *47*, 3084−3086.
(50) Shen, J.; Shi, M.; Yan, B.; Ma, H.; Li, N.; Ye, M. *J. Mater. Chem.* **2011**, *21*, 7795−7801.
(51) Pasricha, R.; Gupta, S.; Srivastava, A. K. *Small* **2009**, *5*, 2253−2259.
(52) Xu, C.; Wang, X. *Small* **2009**, *5*, 2212−2217.
(53) Zhang, S.; Shao, Y.; Liao, H.-g.; Liu, J.; Aksay, I. A.; Yin, G.; Lin, Y. *Chem. Mater.* **2011**, *23*, 1079−1081.
(54) Guo, S.; Wen, D.; Zhai, Y.; Dong, S.; Wang, E. *ACS Nano* **2010**, *4*, 3959−3968.
(55) Zhu, C.; Guo, S.; Zhai, Y.; Dong, S. *Langmuir* **2010**, *26*, 7614−7618.
(56) Zhu, X.; Zhu, Y.; Murali, S.; Stollers, M. D.; Ruoff, R. S. *ACS Nano* **2011**, *5*, 3333−3338.
(57) Zeng, J.; Zhang, Q.; Chen, J.; Xia, Y. *Nano Lett.* **2010**, *10*, 30−35.
(58) Choi, Y.; Bae, H. S.; Seo, E.; Jang, S.; Park, K. H.; Kim, B.-S. *J. Mater. Chem.* **2011**, *21*, 15431−15436.
(59) Huang, J.; Zhang, L.; Chen, B.; Ji, N.; Chen, F.; Zhang, Y.; Zhang, Z. *Nanoscale* **2010**, *2*, 2733−2738.
(60) Li, J.; Liu, C.-y.; Liu, Y. *J. Mater. Chem.* **2012**, *22*, 8426−8430.
(61) Moon, I. K.; Lee, J.; Ruoff, R. S.; Lee, H. *Nat. Commun.* **2010**, *1*.
(62) Zhang, J.; Yang, H.; Shen, G.; Cheng, P.; Zhang, J.; Guo, S. *Chem. Commun.* **2010**, *46*, 1112−1114.
(63) Jana, D.; Dandapat, A.; De, G. *Langmuir* **2010**, *26*, 12177−12184.
(64) Qiu, L.; Peng, Y.; Liu, B.; Lin, B.; Peng, Y.; Malik, M. J.; Yan, F. *Appl. Catal., A* **2012**, *413*− *414*, 230−237.
(65) Kim, J. H.; Boote, B. W.; Pham, J. A.; Hu, J.; Byun, H. *Nanotechnology* **2012**, *23*, 275606.